Title: Performance analysis of asynchronous best-effort traffic   coexisting with TDM reservations in Polymorphous OBS networks

Corresponding Author: Dr. Jose Alberto Hernandez, Ph.D.

Corresponding Author's Institution: Universidad Autónoma de Madrid

First Author: Jose Alberto Hernandez, Ph.D.

Order of Authors: Jose Alberto Hernandez, Ph.D.; Javier Aracil, Ph.D.; Víctor López, MSc; José Luis García Dorado, MSc; Luis de Pedro, Ph.D.

Performance analysis of asynchronous best-effort traffic coexisting with TDM reservations in Polymorphous OBS networks

José Alberto Hernández, Javier Aracil, Víctor López,
José Luis García-Dorado and Luis de Pedro
Networking Research Group, Escuela Politécnica Superior
Universidad Autónoma de Madrid
Calle Francisco Tomás y Valiente 11, 28049 Madrid, Spain

July 7, 2008

Abstract

The in-advance reservation of bandwidth capacity philosophy of Optical Burst Switching architectures via Burst-Control Packets brings high flexibility in the separation of network resources for services with different Quality-of-Service requirements. In this light, real-time applications can periodically be guaranteed a certain amount of bandwidth reservation for the transmission of traffic with Constant Bit Rate requirements (for instance IP Television, VoIP, etc), whilst the remaining capacity may be used for transmission of best-effort traffic of the so-called elastic applications (emailing, web browsing, etc). The Polymorphous, Agile and Transparent Optical Networks (PATON) architecture [1] proposes periodic reservation of time-slots over one or several wavelengths of an optical fibre, yet remaining gaps in between them for transmission of best-effort traffic.

This work presents a novel analysis of the performance perceived by best-effort traffic which are given full access to optical switching only during a portion of the total time. The following analyses the non-blocking probability among best-effort data bursts that share such available gaps in between the periods of CBR traffic. An exact expression of the non-blocking probability is derived when a single wavelength is used for CBR traffic, along with a lower bound for the case when CBR traffic is transmitted using multiple wavelengths. These results can be of further interest in the optimal design of OBS architectures where the transmission of high-priority real-time traffic and best-effort data coexist over the same wavelength.

Keywords: Optical Burst Switching, IP Television, Service differentiation, CBR traffic.

1   Introduction

The Dense Wavelength Division Multiplexing (DWDM) technique [2] for optical data switching enables the possibility of data transmission of up to hundreds of Gbps over the same optical fibre [3]. Optical Burst Switching (OBS) technology allows a high-level utilisation of the optical bandwidth at a moderate cost complexity by aggregation of incoming packets into larger units called data bursts and their further all-optical transmission across the network [4, 5].

In OBS employing JET signalling [6], a wavelength transmission time is reserved in advanced via the so-called Burst-Control Packet (BCP). The BCP is sent an offset time ahead to configure the

core nodes in the source-destination path. Such an in-advance reservation nature of OBS brings high flexibility in the separation of network resources for services with different QoS requirements. This is the key idea of the recent proposal of Polymorphous, Agile and Transparent Optical Networks (PATON) architecture [1], a new optical architecture that allows not only to establish lightpaths just like in Optical Circuit Switching (OCS) or burst services (OBS), but also to perform Time Division Multiplexing (TDM) circuits with subwavelength capacity. Fig. 1 illustrates a core Polymorphous OBS (POBS) node which deals with TDM reservation (synchronous fixed time slots reserved, denoted by 1), a complete wavelength reservation (full wavelength capacity reserved, denoted by 2) and asynchronous traffic bursts (single asynchronous reservations, denoted by 3).
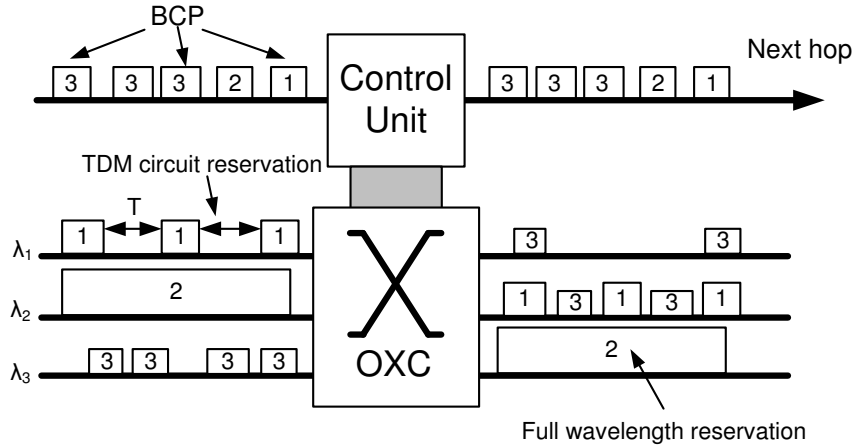

Figure 1: PATON architecture

In PATON, the Burst Control Packets have some common information for all kind of services (such as routing information, initial and final time slot, and offset value), but also they contain specific information for each particular service, such as the reservation period and length for such TDM services. Hence, with the PATON architecture, disparate services, say audio, video, grid and storage, may coexist over the same underlying network infrastructure. Furthermore, services with different reservation strategies can be assigned resources over the same wavelength, as shown in Fig. 1. Additionally, the reservation mechanism may vary depending on the service. For instance, for TDM traffic it is necessary to apply a two-way reservation algorithm, whereas one-way reservation mechanisms suffice for oportunistic Best-Effort data bursts.

For instance, let us consider the case of network operators which are willing to provide an IP Television (IPTV) service to their customers. Typically, this service would require a periodic reservation of bandwidth for the transmission of the video content. This could be addressed by the periodic reservation of a TDM circuit over a single wavelength. Given the high-capacity provided by every wavelength, the gaps in between such periodic reservations could be used for the transmission of OBS best-effort traffic. It is then interesting to study the performance perceived by such best-effort data bursts, assuming that the TDM circuit is given preference. However, to the best of the authors' knowledge, there is no related study concerning this matter.

A number of optical-based technologies have been proposed to combine both periodic TDM reservations with asynchronous best-effort traffic, see for instance the Synchronous OBS (SOBS) [7], Wavelength-Routed OBS (WR-OBS) [8], and Synchronous-Stream OBS (SS-OBS) [9]. The main aspects of SOBS are included in the PATON architecture, except the fact that SOBS does not

permit complete wavelength reservations, just like OCS. On the other hand, WR-OBS assumes two-way reservation mechanism with no wavelength conversion capabilities, hence very different from the PATON architecture. Finally, SS-OBS only considers synchronous reservations, whereby both synchronous and asynchronous traffic is aggregated into synchronous optical bursts.

Thus, all these three technologies are different from the PATON technology since none of them cover all the aspects and services of PATON, say full wavelength reservation, sub-wavelength synchronous reservations and asynchronous best-effort traffic within the same architecture. For this reason, the forthcoming performance analysis is focused on the PATON architecture shown in Fig. 1.

Concerning performance analysis, in [7], the authors realise that generally the data payload is very small compared to the setup time of the switch fabric, and address the problem of grooming of both synchronous and asynchronous data bursts using Fiber Delay Lines (FDLs) in attempt to maintain a high level of network utilisation. Then, the throughput of both types of traffic is evaluated for different grooming policies via simulation, but no analytical study was performed. In our approach, we assume no FDLs are provided.

The following presents a novel analytical study of the performance perceived by the best-effort traffic, while it shares wavelength capacity with periodic reservations. The remainder of this work is thus organised as follows: Section 2 provides a detailed mathematical study of the non-blocking probability perceived by the best-effort traffic. Section 3 aims to show the validity of the equations obtained with simulated results. Finally, Section 4 concludes this work with a brief discussion and final remarks.

2 Analysis

2.1 Notation and preliminaries

The following studies the non-blocking probability of best-effort data bursts that arrive in the gaps between two periods of TDM data transmission over a M-wavelength optical fibre. Such TDM-reserved periods are assumed to be of length T_{on}, whereas the empty gaps between them are denoted by either T_{off} or just T. The data bursts are assumed to be generated by a size-based burst assembler [10, 11], which outputs data bursts of fixed-size B bytes. For convenience, $D = B/C$ shall denote the transmission time of a data burst of B bytes over a wavelength of capacity C bytes/sec.

For instance, Fig. 2 shows the case of three data bursts arriving between two on-time intervals, over the same wavelength. In what follows, x_i shall refer to the arrival time of the i-th data burst, sorted such that $x_1 < x_2 < \ldots < x_n$ assuming n arrivals. In this example, no blocking occurs between any of the three data bursts, since $x_2 > x_1 + D$ and $x_3 > x_2 + D$.
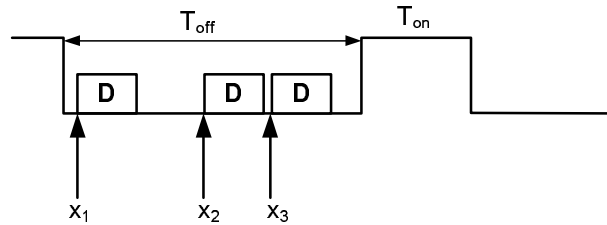

Figure 2: Example of three data bursts arriving in between two TDM reserved periods

Let n refer to the number of packets arriving within an off-time interval of length T. Assuming data bursts arrive following a Poissonian basis (often true for highly multiplexed traffic at small timescales [12]), the probability to have exactly n burst arrivals is given by

$$P(N = n) = \frac{(\lambda T)^n}{n!} e^{-\lambda T}, \quad n = 0, 1, \ldots \tag{1}$$

Under the assumption of n burst arrivals, the joint probability density function of the n arrivals over a period of time T is given by

$$f_n(x_1, \ldots, x_n) = \frac{n!}{T^n} \tag{2}$$

and the probability density function of the k-th arrival ($k = 1, \ldots, n$) is given by order statistics [13]

$$f_{x_k}(x) = \frac{n!}{(k-1)!(n-k)!} \frac{1}{T} \left(\frac{x}{T}\right)^{k-1} \left(\frac{T-x}{T}\right)^{n-k} \tag{3}$$

Additionally, it is worth noticing that the k-th data burst arrives before time τ with probability

$$
\begin{aligned}
P(x_k < \tau) &= \int_0^\tau f_{x_k}(x) dx \\
&= \int_0^\tau \frac{n!}{(k-1)!(n-k)!} \frac{1}{T} \left(\frac{x}{T}\right)^{k-1} \left(\frac{T-x}{T}\right)^{n-k} dx \\
&= \frac{B_{\frac{\tau}{T}}(k, n+1-k)}{B(k, n+1-k)} \tag{4}
\end{aligned}
$$

where $B(a, b)$ refers to the beta function, and $B_x(a, b)$ denotes the incomplete beta function evaluated at x. This is

$$
\begin{aligned}
B(a, b) &= \frac{\Gamma(a)\Gamma(b)}{\Gamma(a+b)} = \frac{(a-1)!(b-1)!}{(a+b-1)!} \tag{5} \\
B_x(a, b) &= \int_0^x u^{a-1}(1-u)^{b-1} du \tag{6}
\end{aligned}
$$

With these former assumptions, the following provides: (1) an exact equation for the non-blocking probability between data bursts over a one-wavelength ($M = 1$) optical fibre; and, (2) a lower bound for the non-blocking probability when several wavelengths are available ($M > 1$).

2.2 Case for a single wavelength

The non-blocking probability of n D-sized optical burst arrivals over a period of time T gives the *probability to have such n bursts successfully allocated within $[0, T]$, that is, none of them overlap with any of the others.* This metric is rather different than the well-known blocking probability since the latter gives the probability to have a given random arrival blocked, and it is easier to derive analytically.

Actually, the analysis of such non-blocking probability arises by integrating the joint-probability distribution of n arrivals (Eq. 2) over the appropriate time intervals:

Let p_n denote the non-blocking probability of n arrivals over $[0, T]$. For $n = 1$ arrival, such non-blocking probability is given by

$$p_1 = \int_0^{T-D} f_1(x_1) dx_1 = \int_0^{T-D} \frac{1}{T} dx_1 = \frac{T-D}{T} \tag{7}$$

Note that the integral range for x_1 is $[0, T-D]$, since if $x_1 \in [T-D, T]$ the data burst is blocked by the subsequent TDM reservation (see Fig. 3).
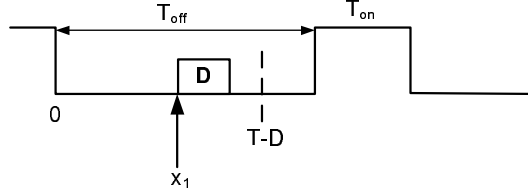

Figure 3: Case of $n = 1$ arrival $(M = 1)$

For $n = 2$ arrivals, the non-blocking probability among bursts is given by

$$
\begin{aligned}
p_2 &= \int_D^{T-D} dx_2 \int_0^{x_2-D} f_2(x_1, x_2) dx_1 = \int_D^{T-D} dx_2 \int_0^{x_2-D} \frac{2!}{T^2} dx_1 = \\
&= \frac{2!}{T^2} \int_D^{T-D} (x_2 - D) dx_2 = \frac{2!}{T^2} \frac{(T-2D)^2}{2} = \left(\frac{T-2D}{T} \right)^2
\end{aligned}
\tag{8}
$$

It is worth noticing that the first data burst must not arrive after $x_2 - D$, otherwise it contends with the second burst. Additionally, the second burst must arrive before $T - D$ in order to avoid contention with the subsequent TDM period, and it also must not arrive before D since it must leave a gap for the first data burst (see Fig. 4). This explains the integral limits $[0, x_2 - D]$ for x_1 and $[D, T - D]$ for x_2.
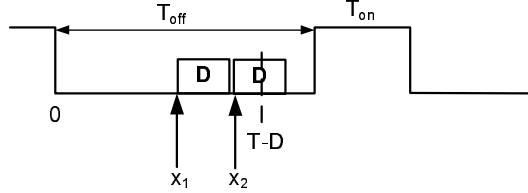

Figure 4: Case of $n = 2$ arrivals $(M = 1)$

Similarly, for $n = 3$ arrivals

$$
\begin{aligned}
p_3 &= \int_{2D}^{T-D} dx_3 \int_D^{x_3-D} dx_2 \int_0^{x_2-D} \frac{3!}{T^3} dx_1 = \frac{3!}{T^3} \int_{2D}^{T-D} dx_3 \int_D^{x_3-D} (x_2 - D) dx_2 = \\
&= \frac{3!}{T^3} \int_{2D}^{T-D} \frac{(x_3 - 2D)^2}{2} dx_3 = \frac{3!}{T^3} \frac{(T-3D)^3}{2 \cdot 3} = \left(\frac{T-3D}{T} \right)^3
\end{aligned}
\tag{9}
$$

Following this reasoning, for any number of arrivals n, it can be shown that

$$
p_n = \left(\frac{T - nD}{T} \right)^n
\tag{10}
$$

Finally, since the number n of burst arrivals follows a Poisson process with rate λ, the total non-blocking probability must take into account the probability of each case above, times the probability of such case to occur, that is, such number of bursts n to arrive. This is

$$P_{\text{nb},M=1} = \sum_{n=0}^{\lfloor \frac{T}{D} \rfloor} \left(\frac{T - nD}{T} \right)^n \frac{(\lambda T)^n}{n!} e^{-\lambda T} = \sum_{n=0}^{\lfloor \frac{T}{D} \rfloor} \frac{(\lambda(T - nD))^n}{n!} e^{-\lambda T} \tag{11}$$

The sum above only takes into account the case of up to $n = \lfloor \frac{T}{D} \rfloor$ arrivals. This is because when more than such number of bursts happen to arrive, two or more bursts will certainly contend.

The following considers the case where multiple wavelengths are available for the transmission of asynchronous best-effort traffic, which are allocated following a round-robin fashion.

2.3   Case for multiple wavelengths with round-robin allocation

This section provides a lower bound of the non-blocking probability when multiple wavelengths are available for the allocation of best-effort traffic, that is, the probability to have a set of n arrivals and none of them contend with any of the others when $M > 1$ wavelengths are available. Essentially, this lower bound is based on the fact that, given n, $0 \leq n \leq M\lfloor \frac{T}{D} \rfloor$ arrivals and M wavelengths, there is no blocking if the x_{k+M} burst arrives D units of time after the arrival of x_k, which means $x_{k+M} > x_k + D$, for all $k = 1, \ldots, n-M$. Again, it is important to note that the arrivals are *sorted*, namely $x_1 \leq x_2 \leq \ldots \leq x_n$.

For instance, let us assume that the TDM traffic uses two wavelengths, as shown in Fig. 5. Let n refer to the number of burst arrivals, and let us consider a round-robin policy for the allocation of data bursts on each wavelength. Following this, the first burst shall be allocated over the first wavelength, and the second arrival shall go to the second wavelength. After this, the third arrival shall be allocated over the first wavelength again, because it is more likely to find it empty than to find the second wavelength available, since the first data burst arrived earlier than the second one. Following this reasoning, the forth burst arrival shall go to the second wavelength again, and so on.

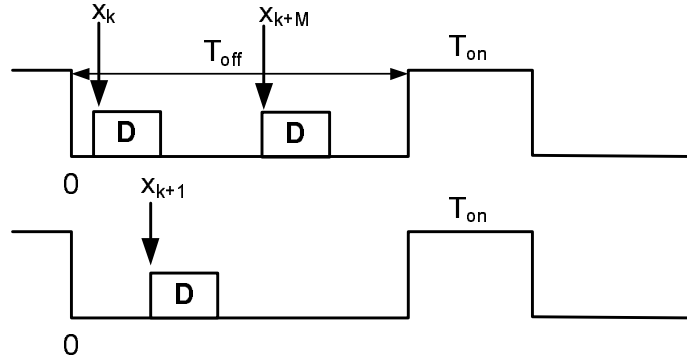
Figure 5: Example of three data bursts arriving to a $M = 2$-wavelength optical fibre

Hence, no blocking occurs in the fibre if the x_k and the x_{k+M} arrivals do not contend, for all k ranging $k = 1, \ldots, n-M$. The conditions to be met by the x_k arrival values for $k = n-M+1, \ldots, n$ are rather different, and just consist on arriving earlier than $T - D$. For clarity, each of these individual probabilities shall be denoted as p_k. That is, p_k stands for the probability that burst k does not contend with burst $k + M$.

First, let us analyse the blocking probability between x_k and x_{k+M}, for $k = 1, \ldots, n - M$. To do so, let y refer to the arrival time of the k-th burst, x_k. As shown previously, its probability density function (PDF) follows

$$f_{x_k}(y) = \frac{(n-k)!}{(k-1)!(n-k)!}\frac{1}{T}\left(\frac{y}{T}\right)^{k-1}\left(\frac{T-y}{T}\right)^{n-k} \tag{12}$$

Assuming this, there is blocking if the $k+M$-th data burst arrives before $y+D$ (see Fig. 6). The probability density function of the $k+M$-th data burst, assuming the k-th burst arrives at time $t=y$ is given by

$$
\begin{aligned}
f_{x_{k+M}|x_k=y}(x) &= \frac{(n-k)!}{(M-1)!(n+1-k-M)!} \\
&\times \frac{1}{T-y}\left(\frac{x}{T-y}\right)^{M-1}\left(\frac{T-y-x}{T-y}\right)^{n-k-M}
\end{aligned} \tag{13}
$$

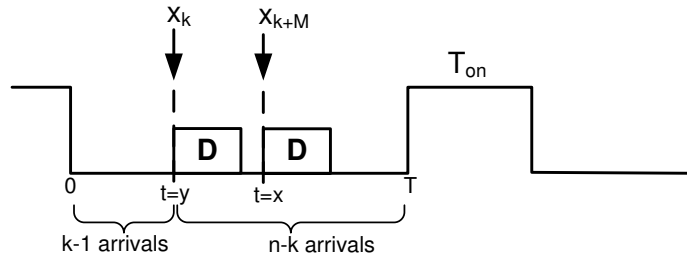which accounts for the PDF of the M-th arrival in a set of $n-k$ over the interval $[0, T-y]$ (see Fig. 6).

Figure 6: Notation for the x_k and the x_{k+M} arrivals

Therefore, there is no blocking between the k-th and the $k+M$-th bursts if there is a gap of at least D units of time between them, that is, with probability

$$
\begin{aligned}
\int_D^{T-y} f_{x_{k+M}|x_k=y}(x)dx &= 1 - \int_0^D f_{x_{k+M}|x_k=y}(x)dx \\
&= 1 - \frac{B_{\frac{D}{T-y}}(M, n+1-k-M)}{B(M, n+1-k-M)}
\end{aligned} \tag{14}
$$

The above provides the non-blocking probability between x_k and x_{k+M} assuming that x_k arrives at time $t=y$. However, we must take into account the non-blocking probability assuming all the possible time arrivals for x_k, in other words, to evaluate such probability for any of the possible values of y. Hence

$$p_k = \int_{y_{\text{ini}}^k}^{y_{\text{fin}}^k} \frac{1}{B(k, n+1-k)} \frac{1}{T} \left(\frac{y}{T}\right)^{k-1} \left(\frac{T-y}{T}\right)^{n-k} \left(1 - \frac{B_{\frac{D}{T-y}}(M, n+1-k-M)}{B(M, n+1-k-M)}\right) dy$$

$$= \int_{y_{\text{ini}}^k}^{y_{\text{fin}}^k} \frac{1}{B(k, n+1-k)} \frac{1}{T} \left(\frac{y}{T}\right)^{k-1} \left(\frac{T-y}{T}\right)^{n-k} dy -$$

$$- \int_{y_{\text{ini}}^k}^{y_{\text{fin}}^k} \frac{1}{B(k, n+1-k)} \frac{1}{T} \left(\frac{y}{T}\right)^{k-1} \left(\frac{T-y}{T}\right)^{n-k} \frac{B_{\frac{D}{T-y}}(M, n+1-k-M)}{B(M, n+1-k-M)} dy =$$

$$= I_1 - I_2 \tag{15}$$

The values of y_{ini}^k and y_{fin}^k are explained in Section 2.4. For now, we only assume that y_{ini}^k refers to the minimum possible arrival value and y_{fin}^k to the maximum arrival value for x_k such that no blocking occurs.

Solving both integrals (I_1 and I_2) separately yields

$$I_1 = \int_{y_{\text{ini}}^k}^{y_{\text{fin}}^k} \frac{1}{B(k, n+1-k)} \frac{1}{T} \left(\frac{y}{T}\right)^{k-1} \left(\frac{T-y}{T}\right)^{n-k} dy$$

$$= \frac{1}{B(k, n+1-k)} \left(B_{\frac{y_{\text{fin}}^k}{T}}(k, n+1-k) - B_{\frac{y_{\text{ini}}^k}{T}}(k, n+1-k)\right) \tag{16}$$

and

$$I_2 = \int_{y_{\text{ini}}^k}^{y_{\text{fin}}^k} \frac{1}{B(k, n+1-k)} \frac{1}{T} \left(\frac{y}{T}\right)^{k-1} \left(\frac{T-y}{T}\right)^{n-k} \frac{B_{\frac{D}{T-y}}(M, n+1-k-M)}{B(M, n+1-k-M)} dy \tag{17}$$

To proceed with I_2, we shall note that the incomplete beta function can be reformulated as

$$B_x(a, b) = x^a \left(\frac{1}{a} + \sum_{i=1}^{b-1} \frac{\prod_{j=1}^{i}(j-b)}{i!(a+i)} x^i\right), \quad a \in Z^+ \tag{18}$$

Following this

$$I_2 = \frac{1}{B(k, n+1-k)B(M, b)} I_2' \tag{19}$$

where $b = n+1-k-M$. I_2' is thus given by

$$I_2' = \int_{y_{\text{ini}}^k}^{y_{\text{fin}}^k} \frac{1}{T} \left(\frac{y}{T}\right)^{k-1} \left(\frac{T-y}{T}\right)^{n-k} \left(\frac{D}{T-y}\right)^M \left(\frac{1}{M} + \sum_{i=1}^{b-1} \frac{\prod_{j=1}^{i}(j-b)}{i!(M+i)} \left(\frac{D}{T-y}\right)^i\right) dy$$

$$= \int_{y_{\text{ini}}^k}^{y_{\text{fin}}^k} \frac{1}{T} \left(\frac{y}{T}\right)^{k-1} \left(\frac{T-y}{T}\right)^{n-k-M} \left(\frac{D}{T}\right)^M \frac{1}{M} dy + \tag{20}$$

$$+ \int_{y_{\text{ini}}^k}^{y_{\text{fin}}^k} \frac{1}{T} \left(\frac{y}{T}\right)^{k-1} \left(\frac{T-y}{T}\right)^{n-k-M} \left(\frac{D}{T}\right)^M \sum_{i=1}^{b-1} \frac{\prod_{j=1}^{i}(j-b)}{i!(M+i)} \left(\frac{D}{T-y}\right)^i dy \tag{21}$$

$$= I_{21}' + I_{22}'$$

Again, solving both (I'_{21} and I'_{22}) separately

$$
\begin{aligned}
I'_{21} &= \int_{y^k_{\text{ini}}}^{y^k_{\text{fin}}} \frac{1}{T} \left(\frac{y}{T}\right)^{k-1} \left(\frac{T-y}{T}\right)^{n-k-M} \left(\frac{D}{T}\right)^{M} \frac{1}{M} dy \\
&= \frac{1}{M} \left(\frac{D}{T}\right)^{M} \left(B_{\frac{y^k_{\text{fin}}}{T}}(k,b) - B_{\frac{y^k_{\text{ini}}}{T}}(k,b) \right)
\end{aligned}
\tag{22}
$$

and

$$
\begin{aligned}
I'_{22} &= \sum_{i=1}^{b-1} \frac{\prod_{j=1}^{i}(j-b)}{i!(M+i)} \left(\frac{D}{T}\right)^{M+i} \int_{y^k_{\text{ini}}}^{y^k_{\text{fin}}} \frac{1}{T} \left(\frac{y}{T}\right)^{k-1} \left(\frac{T-y}{T}\right)^{n-k-M-i} dy \\
&= \sum_{i=1}^{b-1} \frac{\prod_{j=1}^{i}(j-b)}{i!(M+i)} \left(\frac{D}{T}\right)^{M+i} \left(B_{\frac{y^k_{\text{fin}}}{T}}(k,b-i) - B_{\frac{y^k_{\text{ini}}}{T}}(k,b-i) \right)
\end{aligned}
\tag{23}
$$

All the equations above together yield

$$
\begin{aligned}
p_k &= \frac{1}{B(k,n+1-k)} \left(B_{\frac{y^k_{\text{fin}}}{T}}(k,n+1-k) - B_{\frac{y^k_{\text{ini}}}{T}}(k,n+1-k) \right) - \\
&\quad - \frac{1}{B(k,n+1-k)B(M,b)} \frac{1}{M} \left(\frac{D}{T}\right)^{M} \left(B_{\frac{y^k_{\text{fin}}}{T}}(k,b) - B_{\frac{y^k_{\text{ini}}}{T}}(k,b) \right) \\
&\quad - \frac{1}{B(k,n+1-k)B(M,b)} \sum_{i=1}^{b-1} \frac{\prod_{j=1}^{i}(j-b)}{i!(M+i)} \left(\frac{D}{T}\right)^{M+i} \left(B_{\frac{y^k_{\text{fin}}}{T}}(k,b-i) - B_{\frac{y^k_{\text{ini}}}{T}}(k,b-i) \right) \\
&\quad \text{for } k < n - M
\end{aligned}
\tag{24}
$$

where $b = n + 1 - k - M$.

The values of p_k for $k = M - n, \ldots, n$ are much easier to obtain, since the k-th arrival only needs to be checked whether or not it arrives before $T - D$ giving

$$
p_k = \frac{B_{\frac{T-D}{T}}(k,n+1-k) - B_{\frac{y^k_{\text{ini}}}{T}}(k,n+1-k)}{B(k,n+1-k)} \quad \text{for } k > n - M
\tag{25}
$$

2.4   Values for y^k_{ini} and y^k_{fin}

As stated before, the non-blocking probability has been obtained by integrating the joint probability density function of x_k and x_{k+M}, over the range of values y^k_{ini} to y^k_{fin}. The reason for this is that x_k cannot take every possible value in the range $[0, T]$, since some values may produce blocking.

For instance, if $M = 3$, x_1, x_2 and x_3 may arrive at time $t = 0$ and onwards, since x_1 will be allocated on the first wavelength, x_2 on the second one, and x_3 on the third one. Thus $y^k_{\text{ini}} = 0$ for all of them. However, the fourth arrival x_4 should not arrive before time $y^k_{\text{ini}} = D$, because it would be allocated on wavelength number one and must leave at least a gap of D for x_1. The same reasoning applies to x_5 and x_6, which must have $y^k_{\text{ini}} = D$. Similarly, the value of y^k_{ini} for x_7, x_8 and x_9 would be $y^k_{\text{ini}} = 2D$, and so forth. Finally, for any value of k and M, y^k_{ini} is given by

$$y_{\text{ini}}^k = \lfloor \frac{k-1}{M} \rfloor D, \quad k = 1, 2, \ldots, n \tag{26}$$

The same reasoning applies to y_{fin}^k, which yields

$$y_{\text{fin}}^k = T - \lceil \frac{n-k+1}{M} \rceil D, \quad k = 1, 2, \ldots, n \tag{27}$$

2.5 Lower bound

Note that the integration limits derived above produce a best-case non-blocking probability. Actually, the integration region defined by the former limits is $\mathbb{S} = \{y_{\text{ini}}^k \leq x_k \geq y_{\text{fin}}^k, 1 \leq k \leq n\}$, whereas the real integration region is $\mathbb{S}' = \{x_1 \leq x_2 \leq \ldots \leq x_n, 1 \leq k \leq n\}$, which is smaller. Consequently, the product

$$L_b^{(n)} = \prod_{k=1}^n p_k \tag{28}$$

provides a lower bound, which can be used to derive the following non-blocking probability lower bound

$$P_{\text{nb}, M>1} \geq \sum_{n=0}^{M \lfloor \frac{T}{D} \rfloor} L_b^{(n)} \frac{\lambda T}{n!} e^{-\lambda T} \tag{29}$$

under the assumption of Poissonian burst arrivals with rate λ.

The experiments section investigates the accuracy of such approximation and shows the conditions under which the lower bound approaches the real values.

2.6 Bursts arriving during the on-interval

As stated in the introduction we assume that no optical buffering is available, hence, data bursts arriving during the on-intervals are dropped. The non-blocking probability as derived above does not take into account this issue. Essentially, the non-blocking probability in the on-period is simply given by the probability of no arrivals in a Poisson process during T_{on}, that is: $e^{-\lambda T_{\text{on}}}$. Thus, the total non-blocking probability is the product of both non-blocking probabilities in the on- and off-intervals.

3 Experiments and results

The next experiments aim to validate the exact equation for the non-blocking probability derived in Section 2.2, and to assess on the validity of the lower bound obtained in Section 2.3 as a possible approximation for the non-blocking probability for cases where multiple wavelengths use TDM reservations.

3.1 Scenario definition

In the following, we assess the validity of the equations obtained above in a scenario whereby an ISP provider is willing to provide IP Television (IPTV) to its customers using the PATON architecture. At present, a number of ISP providers are currently providing IPTV over ADSL.

Basically, we use the following parameters, which have been obtained from a trace kindly donated by one of such IPTV providers. Such trace showed a number of MPEG-2 encoded TV channels with a bitrate of 4.16 Mbps per channel, according to the Standard Definition Television (SDTV) [14]. Also, each TV channel appeared as a Constant Bit Rate (CBR) stream with packet interarrival times of 2.5 ms. In the following, we assume $N_{ch} = 192$ as the number of TV channels to be transmitted over a fibre length with $M \in \{1, 2, 4, 8\}$ wavelengths of 10 Gbps capacity.

In this example, the bandwidth consumed by the TDM reservations is

$$192 \text{ channels} \times 4.16 \text{ Mbps/channel} = 798.72 \text{ Mbps}$$

If allocated in a single wavelength, this amount constitutes

$$\frac{798.72 \text{ Mbps}}{10 \text{ Gbps}} \approx 8\%$$

of its total capacity.

If allocated over M wavelengths, the amount above should be divided by M. As shown, a typical TDM service of IPTV provisioning only comprises a small portion of the total amount of bandwidth available in an optical fibre, and it makes sense to fulfill the remaining capacity with best-effort asynchronous traffic, as noted in [1].

Fig. 7 shows the values of T_{on} and T_{off} in a scenario where the 192 TV channels are allocated over a single wavelength (left), or split into $M = 4$ wavelengths (right). For $M = 1$, the calculus is as follows
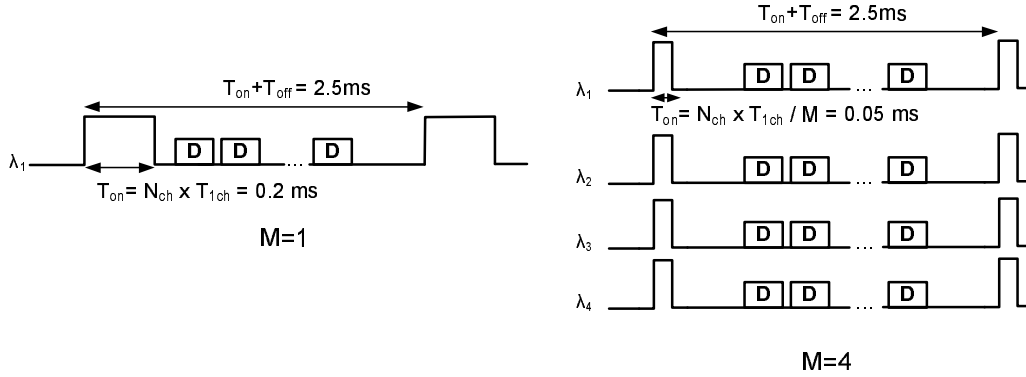

Figure 7: Allocation of 192 IPTV channels in a single wavelength (left), and over four wavelengths (right)

$$T_{on} = 2.5 \text{ ms} \times 8\% = 0.2 \text{ ms}$$

$$T_{off} = 2.5 \text{ ms} \times 92\% = 2.3 \text{ ms}$$

For any value of M, this is

$$T_{on} = 2.5 \text{ ms} \times \frac{N_{ch} \cdot 4.16 \text{ Mbps}}{M \cdot C}$$

$$T_{off} = 2.5 \text{ ms} - T_{on}$$

Concerning the size of asynchronous best-effort data bursts D, we assume that bursts aggregate a number of $N_{\text{packets}} \in \{150, 300, 600\}$ packets of 1024 bytes/packet on average. For the case of $N_{\text{packets}} = 150$ packets, this gives

$$D = \frac{150 \times 1024 \cdot 8 \text{ bits/burst}}{10 \text{ Gbps}} \approx 0.125 \text{ ms}$$

Finally, we denote ρ as the utilisation factor for such best-effort traffic

$$\rho = \frac{\lambda D}{M}$$

assuming data bursts arrive following a Poisson process with rate λ bursts/sec.

3.2 Numerical example for $M = 1$

This experiment assumes $T_{\text{off}} = 2.3$ ms and $D \in \{0.025, 0.125, 0.25, 0.5\}$ ms in the single-wavelength example of Fig. 7 (left). Fig. 8 shows the values of p_n in Eq. 10 assuming n arrivals.
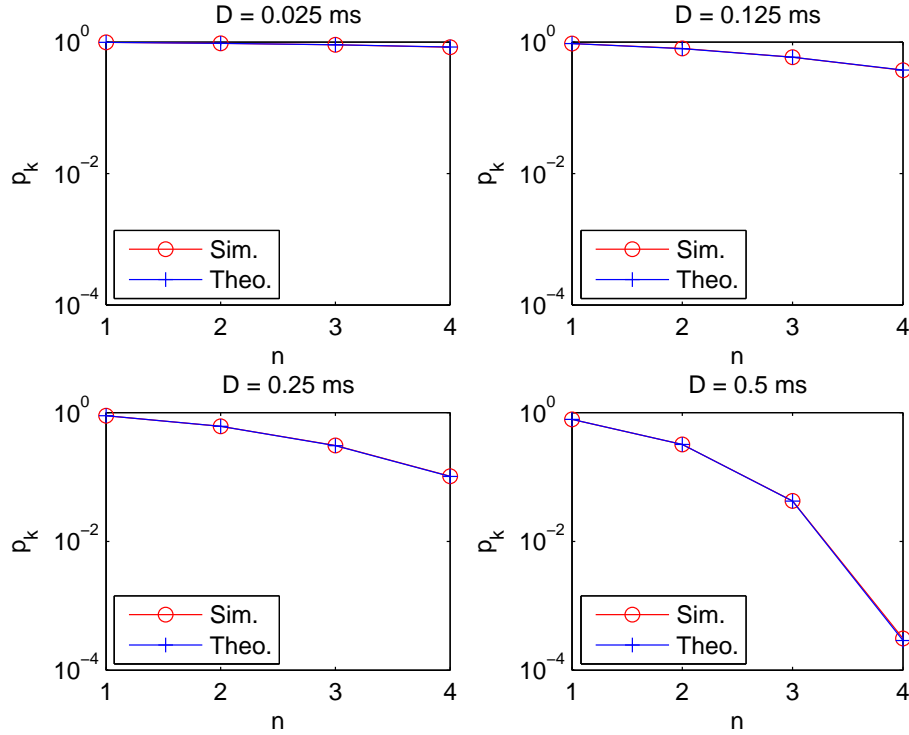

Figure 8: Non-blocking probability with $M = 1$, $T_{\text{off}} = 2.3$ ms and $D = 0.025$ (top-left), $D = 0.125$ (top-right), $D = 0.25$ (bottom-left) and $D = 0.5$ (bottom-right)

Two conclusions arise from this plot: (1) p_n is larger for small bursts, since they are easier to allocate along T_{off}; and (2), the smaller the number of bursts n to fit in T_{off} the better (higher values of p_n).

	$M = 1$, $T_{\text{off}} = 2.3ms$		
	$D = 0.125ms$	$D = 0.25ms$	$D = 0.5ms$
$\rho = 0.01$	$p_s = 0.9885$	$p_s = 0.9892$	$p_s = 0.9897$
	$p_{th} = 0.9884$	$p_{th} = 0.9893$	$p_{th} = 0.9897$
$\rho = 0.10$	$p_s = 0.7812$	$p_s = 0.8453$	$p_s = 0.8803$
	$p_{th} = 0.7805$	$p_{th} = 0.8457$	$p_{th} = 0.8803$
$\rho = 0.25$	$p_s = 0.3563$	$p_s = 0.5435$	$p_s = 0.6724$
	$p_{th} = 0.3556$	$p_{th} = 0.5435$	$p_{th} = 0.6719$
$\rho = 0.50$	$p_s = 0.0485$	$p_s = 0.1887$	$p_s = 0.3732$
	$p_{th} = 0.0483$	$p_{th} = 0.1891$	$p_{th} = 0.3740$
$\rho = 0.75$	$p_s = 0.0039$	$p_s = 0.0512$	$p_s = 0.1873$
	$p_{th} = 0.0039$	$p_{th} = 0.0514$	$p_{th} = 0.1870$

Table 1: Simulated and theoretical results obtained for $M = 1$

Table 1 shows the non-blocking probability values obtained via simulation (p_s in the table) and theoretically (p_{th} in the table) for several ρ and D values. As shown, the simulated results match exactly the non-blocking probability values obtained given by Eq. 11.

Clearly, the non-blocking probability decreases for higher utilisation factors, regardless of the values of D. However, under the same load ρ, it is generally easier (higher non-blocking probability) to fit large bursts than smaller ones. The main reason for this is that, although they are larger, these are few in number. The conclusion is that it is preferred to set the burst assemblers at core nodes to output large data bursts since they offer higher non-blocking probability.

3.3   Numerical example for $M > 1$

The purpose of this section is two-fold. First, it aims to show the accuracy of the lower bound obtained in the analysis; and secondly, it gives insight into the values of ρ, D and T_{off} for which the lower bound gives an accurate approximation of the actual non-blocking probability.

Fig. 9 shows the values of p_k in a simulation scenario with $M = 2$, $T_{\text{off}} = 2.4$ ms and different values of D, as obtained following Eqs. 24 and 25. The results only show the values of p_k for $k = 1, \ldots, 8$. As shown in the plots, the lower bound always gives a smaller value than the one obtained via simulation. This can be explained in terms of the integration regions considered in Section 2.4. As the number of arrivals grows, the difference between the real and approximate integration regions increases, which results in a larger deviation between the theoretical and simulation results. Additionally, the lower bound approaches the simulated values when the number of burst arrivals is small, and specially, when $D \ll T$.

The same conclusions arise from Fig. 10, where the same experiment was run but for $M = 8$ wavelengths, and assuming up to $n = 32$ arrivals. Again, the lower-bound $L_b^{(n)}$ almost matches the real results for low values of D and of n and separates from it, as any of these two values grows. However, the lower bound is very conservative for small T/D (Fig. 10: top-right, bottom-left, and especially bottom-right).

Concluding, the accuracy of the lower bound $L_b^{(n)}$ depends on three parameters: assumed number of arrivals n, the relationship T/D, and mostly on the number of wavelengths M. In the first case, in low-loaded scenarios (few burst arrivals) the lower bound approximates the real non-blocking probability more accurately than in high-loaded scenarios. In this case (low-loaded scenarios), the lower bound constitutes a good approximation the smaller $\frac{T}{D}$ and the number of wavelengths M,
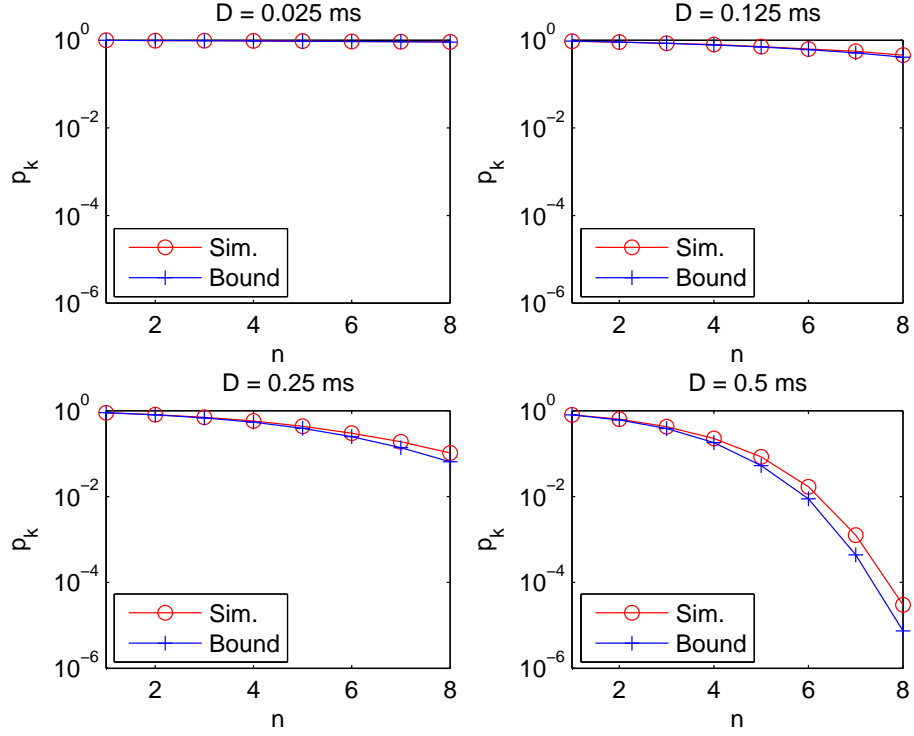
Figure 9: Non-blocking probability with $M = 2$, $T_{\text{off}} = 2.4$ and $D = 0.025$ (top-left), $D = 0.125$ (top-right), $D = 0.25$ (bottom-left) and $D = 0.5$ (bottom-right)
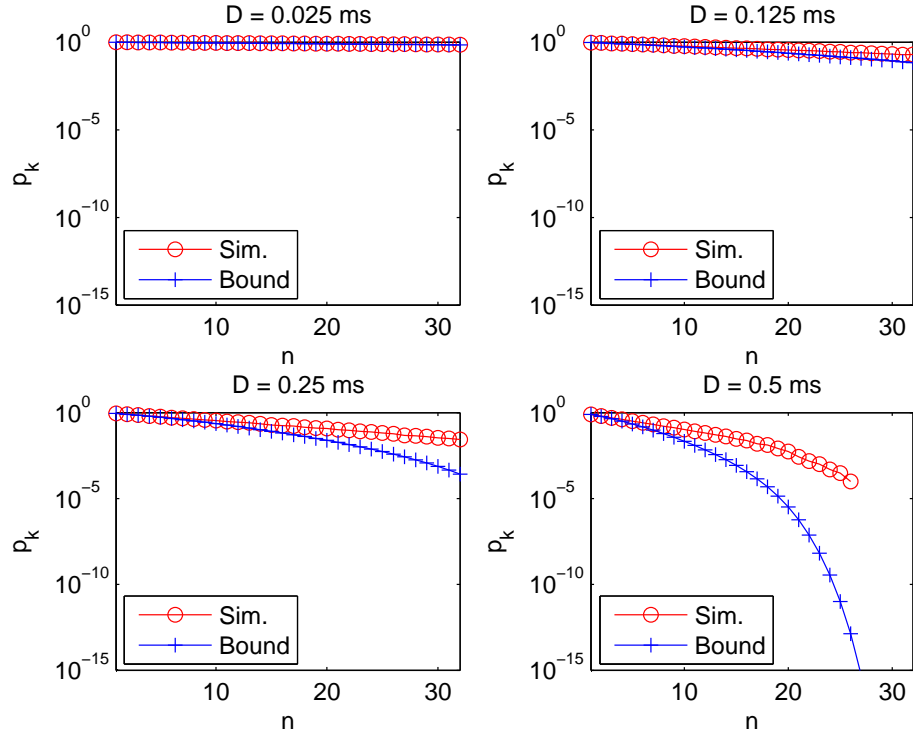
Figure 10: Non-blocking probability with $M = 8$, $T_{\text{off}} = 2.475$ and $D = 0.025$ (top-left), $D = 0.125$ (top-right), $D = 0.25$ (bottom-left) and $D = 0.5$ (bottom-right)

since the region of integration considered in the lower bound is closer to the real one (see Section 2.4). Table 2 summarises these ideas.

		$\rho = 0.01$	$\rho = 0.1$	$\rho = 0.25$	$\rho = 0.5$	$\rho = 0.75$
$M = 2$	$D = 0.125$	$p_s = 0.9809$	$p_s = 0.7753$	$p_s = 0.3336$	$p_s = 0.0212$	$p_s = 3.68 \cdot 10^{-4}$
		$L_b = 0.9800$	$L_b = 0.7611$	$L_b = 0.2972$	$L_b = 0.0144$	$L_b = 1.90 \cdot 10^{-4}$
	$D = 0.25$	$p_s = 0.9801$	$p_s = 0.8014$	$p_s = 0.4604$	$p_s = 0.0985$	$p_s = 0.0113$
		$L_b = 0.9800$	$L_b = 0.7878$	$L_b = 0.4299$	$L_b = 0.0793$	$L_b = 7.89 \cdot 10^{-3}$
	$D = 0.5$	$p_s = 0.9804$	$p_s = 0.8094$	$p_s = 0.5472$	$p_s = 0.2137$	$p_s = 0.0639$
		$L_b = 0.9801$	$L_b = 0.8028$	$L_b = 0.5204$	$L_b = 0.1911$	$L_b = 0.0539$
$M = 4$	$D = 0.125$	$p_s = 0.9604$	$p_s = 0.6678$	$p_s = 0.2930$	$p_s = 0.0121$	$p_s = 3.05 \cdot 10^{-5}$
		$L_b = 0.9601$	$L_b = 0.6246$	$L_b = 0.1913$	$L_b = 0.0021$	$L_b = 1.03 \cdot 10^{-6}$
	$D = 0.25$	$p_s = 0.9621$	$p_s = 0.6728$	$p_s = 0.3324$	$p_s = 0.0451$	$p_s = 1.60 \cdot 10^{-3}$
		$L_b = 0.9602$	$L_b = 0.6311$	$L_b = 0.2390$	$L_b = 0.0148$	$L_b = 2.25 \cdot 10^{-4}$
	$D = 0.5$	$p_s = 0.9607$	$p_s = 0.6673$	$p_s = 0.3535$	$p_s = 0.0855$	$p_s = 0.0122$
		$L_b = 0.9603$	$L_b = 0.6400$	$L_b = 0.2787$	$L_b = 0.0437$	$L_b = 3.99 \cdot 10^{-3}$
$M = 8$	$D = 0.125$	$p_s = 0.9809$	$p_s = 0.7753$	$p_s = 0.3336$	$p_s = 0.0212$	$p_s = 3.68 \cdot 10^{-4}$
		$L_b = 0.9205$	$L_b = 0.3524$	$L_b = 0.0345$	$L_b = 2.55 \cdot 10^{-5}$	$L_b = 3.74 \cdot 10^{-11}$
	$D = 0.25$	$p_s = 0.9809$	$p_s = 0.7753$	$p_s = 0.3336$	$p_s = 0.0212$	$p_s = 3.68 \cdot 10^{-4}$
		$L_b = 0.9208$	$L_b = 0.3619$	$L_b = 0.0421$	$L_b = 2.14 \cdot 10^{-4}$	$L_b = 8.23 \cdot 10^{-8}$
	$D = 0.5$	$p_s = 0.9809$	$p_s = 0.7753$	$p_s = 0.3336$	$p_s = 0.0212$	$p_s = 3.68 \cdot 10^{-4}$
		$L_b = 0.9213$	$L_b = 0.3794$	$L_b = 0.0562$	$L_b = 0.0010$	$L_b = 7.30 \cdot 10^{-6}$

Table 2: Simulated and theoretical results obtained for $M = 2$, $M = 4$ and $M = 8$

4   Summary and conclusions

This work presents a novel (possibly first) study of the performance observed by asynchronous best-effort traffic fitted in between the gaps of periodic TDM reservations in the Polymorphous OBS architecture proposed in [1]. Particularly, an exact equation of the non-blocking probability is obtained for a single-wavelength, along with a lower bound when best-effort traffic is allocated following a round-robin policy along multiple wavelengths. The results show that such lower boundary approaches the exact values when the data burst sizes are not much smaller than the gaps in between the TDM reservations, and particularly accurate when a few wavelengths are used in this purpose.

Additionally, the equations have been validated in a scenario whereby an ISP aims to provide IP Television to their customers. The parameters used for the simulation are close to reality and have been derived from a trace donated by one of the Spanish IPTV service providers, thus validating the results in a real scenario. The numerical example shows the feasibility in the coexistance of multiple transmission strategies over DWDM (Polimorphous OBS) given the high-capacity nature of optical fibres. The equations derived can be further applied to the dimensioning and planning of several aspects of such POBS architecture.

The blocking effects can be alleviated by means of buffering blocked bursts and further re-schedule them in subsequent available off-time intervals. The analysis of such a queue has been a matter of study in the past, see [15] and references therein. However, note that the distinguishing feature of this study is the evaluation of non-blocking probabilities during off periods.

Acknowledgements

References

[1] C. Qiao, W. Wei, and X. Liu. Extending generalized multiprotocol label switching (GMPLS) for polymorphous, agile, and transparent optical networks (PATON). *IEEE Comms. Magazine*, 44(12):104–114, Dec 2006.

[2] International Telecommunication Union. Recommendation on DWDM (G.692).

[3] G. Bernstein, B. Rajagopalan, and D. Saha. *Optical Network Control: Architecture, Protocols, and Standards.* Addison-Wesley Professional, 1st edition, July 2003.

[4] C. Qiao and M. Yoo. Optical Burst Switching (OBS) – A new paradigm for an optical Internet. *J. High Speed Networks*, 8:69–84, 1999.

[5] S. Verma, H. Chaskar, and R. Ravikanth. Optical Burst Switching: A viable solution for Terabit IP backbone. *IEEE Network*, Nov/Dec:48–53, 2000.

[6] M. Yoo and C. Qiao. Just-Enough Time (JET): A high-speed protocol for bursty traffic in optical networks. In *Proc. of IEEE/LEOS Conf. Tech. Global Info. Infrastructure*, pages 26–27, Montreal, Canada, Aug. 1997.

[7] S. Sheeshia and C. Qiao. Synchronous optical burst switching. In *Proc. of Broadnets*, pages 4–13, San Jose, California, USA, Oct. 2004.

[8] M. Duser and P. Bayvel. Analysis of wavelength-router optical bursts-switched network performance. In *Proc. of European Conf. Optical Communications*, volume 1, pages 46–47, Amsterdam, The Netherlands, Oct. 2001.

[9] O. Yu and Ming Liao. Synchronous stream optical burst switching. In *Proc. of Broadnets*, pages 1447–1452, Boston, Massachusetts, USA, Oct. 2005.

[10] V. M. Vokkarane, Q. Zhang, J. P. Jue, and B. Chen. Generalized burst assembly and scheduling techniques for QoS support in Optical Burst-Switched networks. In *Proc. of IEEE Globecom*, volume 3, pages 2747– 2751, Taipei, Taiwan, Nov. 2002.

[11] X. Cao, J. Li, Y. Chen, and C. Qiao. Assembling TCP/IP packets in Optical Burst Switched networks. In *Proc. of IEEE Globecom*, volume 3, pages 2808– 2812, Taipei, Taiwan, Nov. 2002.

[12] T. Karagiannis, M. Molle, M. Faloutsos, and A. Broido. A nonstationary Poisson view of Internet traffic. In *Proc. of IEEE Infocom*, volume 3, pages 1558– 1569, Hong Kong, PLC, March 2004.

[13] H. A. David. *Order statistics.* Wiley Series in Probability and Mathematical Statistics. John Wiley & Sons, second edition, 1980.

[14] G. Held. *Understanding IPTV (Informa Telecoms & Media).* Auerbach Publications, Boston, MA, USA, Oct. 2006.

[15] H. Bruneel and B. G. Kim. *Discrete-time models for communication systems including ATM.* Kluwer Academic Publishers, 1993.

* Response to Reviewer Comments

Dear Editor,

These are the main changes in the new version:

- We have used a new template to generate section and subsection indexing as recommented.

- All typos have been fixed.

- Figures 8, 9 and 10 required spacing in their titles. These are now correct.

- Figure 1 has been changed, and now shows a more scientific appearance, as recommended. Figure 6 has also been modified to improve its readability.

- The references have been completed, including the volume numbers of some of them, as proposed.

- The last paragraph of conclusions has been changed as proposed.

* Author Biography (250 words max.)

José Alberto Hernández completed the five-year degree in Telecommunications Engineering at Universidad Carlos III de Madrid (Spain) in 2002, and the Ph.D. degree in Computer Science at Loughborough University (United Kingdom) in 2005. After this, he joined the Networking Research Group at Universidad Autónoma de Madrid (Spain), where he actively participates in a number of both national and european research projects concerning the modeling and performance evaluation of communication networks, and particularly the optical burst switching technology. His research interests include the areas at which mathematical modeling and computer networks overlap.

* Author Biography (250 words max.)

Javier Aracil received the M.Sc. and Ph.D. degrees (Honors) from
Technical University of Madrid in 1993 and 1995, both in
Telecommunications Engineering. In 1995 he was awarded with a
Fulbright scholarship and was appointed as a Postdoctoral Researcher
of the Department of Electrical Engineering and Computer Sciences,
University of California, Berkeley. In 1998 he was a research scholar
at the Center for Advanced Telecommunications, Systems and Services of
The University of Texas at Dallas. He has been an associate professor
for University of Cantabria and Public University of Navarra and he is
currently a full professor at Universidad Autónoma de Madrid, Madrid,
Spain. His research interest are in optical networks and performance
evaluation of communication networks. He has authored more than 50
papers in international conferences and journals.

* Author Biography (250 words max.)

Víctor López Álvarez completed his MSc. degree in Telecommunications Engineering with Honours at Universidad de Alcalá in 2005. Before that in 2004, he joined Telefonica Investigacion y Desarrollo where as a researcher in next generation networks for metro, core and access. During this period, he participated in several European Union projects (NOBEL, MUSE, MUPBED) focused in the previous topics. In 2006, he joined the Networking Research Group of Universidad Autónoma de Madrid as a researcher in ePhoton/One Plus Network of Excelence. His research interests are focused on the analysis and characterization of services, design and performance evaluation of traffic monitoring equipment, and the integration of Internet services over WDM networks, mainly OBS solutions.

* Author Biography (250 words max.)

José Luis García Dorado received the M.Sc. degree in Computer Science
from Universidad Autónoma de Madrid in 2006. After this, he joined the
Networking Research Group, as a researcher in the ePhoton/One+ Network
of Excellence. At present, he participates in DIOR, a national
research project whose aim is to dimension the Spanish National
Research and Educational Network. In 2007 he was awarded with a
four-year fellowship by the Ministry of Science and Education of Spain
(F.P.I scholarship). His research interests are focused on the
analysis of network traffic, its management, monitoring, modelling and
dimensioning.

* Author Biography (250 words max.)

Luis de Pedro completed his MSc. and Ph.D. degrees in Telecommunications Engineering at Universidad Politécnica de Madrid, Spain. In 1997, he joined Hewlett Packard where he has lead a large number of projects concerning e-commerce and Internet banking mostly. Additionally, he is a part-time associate professor at Universidad Autónoma de Madrid, Spain, where he has taught computer networks for more than ten years. His research interests are focused on the performance evaluation of communication networks and optical burst-switched technologies.